

Studying the gradient flow coupling in the Schrödinger functional

DESY 13-150
HU-EP-13/38
SFB/CPP-13-57

P. Fritzs*

*Institut für Physik, Humboldt-Universität zu Berlin,
Newtonstr. 15, 12489 Berlin, Germany
E-mail: fritzs@physik.hu-berlin.de*

A. Ramos

*NIC, DESY,
Platanenallee 6, 15738 Zeuthen, Germany
E-mail: alberto.ramos@desy.de*

We discuss the setup and features of a new definition of the running coupling in the Schrödinger functional scheme based on the gradient flow. Its suitability for a precise continuum limit in QCD is demonstrated on a set of $N_f = 2$ gauge field ensembles in a physical volume of $L \sim 0.4\text{fm}$.

*The 31th International Symposium on Lattice Field Theory - Lattice 2013,
July 29 – August 03, 2013
Mainz, Germany*

*Speaker.

1. Introduction

Some years ago the Yang-Mills gradient flow was introduced to the Lattice Field Theory community by M.Lüscher [1] as an additional tool for studying the dynamics of gauge theories non-perturbatively. Since then the number of applications of the YM gradient flow to probe non-perturbative aspects of non-Abelian gauge theories using old and new ideas steadily increases — as can be seen in the various contributions to this conference for instance. So far most of them are influenced by [1] and the all-order proof in perturbation theory given in [2] which tells us that the gauge field that is generated by the flow equations

$$\frac{dB_\mu(x,t)}{dt} = D_\nu G_{\nu\mu}(x,t), \quad t > 0, \quad (1.1a)$$

$$G_{\mu\nu}(x,t) = \partial_\mu B_\nu - \partial_\nu B_\mu + [B_\mu, B_\nu], \quad D_\nu = \partial_\nu + [B_\nu, \star], \quad (1.1b)$$

$$B_\mu(x,t)|_{t=0} = A_\mu(x), \quad (1.1c)$$

does not require renormalization. Here $A_\mu(x)$ is the fundamental gauge field of the underlying theory and the flow field $B_\mu(x,t)$ is the solution to (1.1a) subject to the initial condition (1.1c). On the lattice the gradient flow is also referred to as Wilson flow if the Wilson plaquette gauge action has been used to define the flow equations in terms of parallel transporters [3, 1]. In that case it has rigorously been shown that the action is a monotonically decreasing function of t and the flow thus represents a smoothing operation of the initial gauge field.

2. Definition of a new coupling

Here we are especially interested in one of the applications that were already mentioned in [1], namely to use the energy density

$$\langle E(t) \rangle \equiv \frac{1}{4} \langle G_{\mu\nu}(t) G_{\mu\nu}(t) \rangle = \frac{3(N^2 - 1)}{2(8\pi t)^2} \times \bar{g}_{\text{MS}}^2(\mu) \left\{ 1 + c_1 \bar{g}_{\text{MS}}^2 + \mathcal{O}(\bar{g}_{\text{MS}}^4) \right\} \quad (2.1)$$

at positive flow time to define a running coupling. This perturbative expansion of the energy density in terms of a renormalized coupling is given for 4 Euclidean space-time dimensions in infinite volume for gauge group $SU(N)$ at scale $\mu = 1/\sqrt{8t}$, where $\sqrt{8t}$ is the mean-square radius over which the gauge field is effectively smoothed. This obviously can serve as a definition of a non-perturbatively renormalized coupling after switching from dimensional regularisation to the lattice as a regulator, leading to the gradient flow coupling

$$\langle t^2 E(t) \rangle \equiv \mathcal{N} \times \bar{g}_{\text{GF}}^2(\mu), \quad \mu = 1/\sqrt{8t} = 1/cL. \quad (2.2)$$

The energy density as a gauge invariant quantity scales $\propto t^{-2}$ and is a renormalized quantity at positive flow time. The normalization constant \mathcal{N} has to be chosen such that $\bar{g}_{\text{GF}}^2 = g_0^2 + \mathcal{O}(g_0^4)$ holds and can be computed by expanding the energy density in the bare gauge coupling as defined through the field strength tensor $G_{\mu\nu}(t)$. In a finite volume one has the additional length scale L , the physical size of a hypercube with volume $V = L^4$, which in a finite size scaling procedure usually sets the renormalization scale in some well-defined way. It is necessary to fix the factor $c = \sqrt{8t}/L$ that defines the effective smoothing range in terms of the physical extent.

In a finite volume, boundary conditions of the field variables become important and the energy density has in fact already been used to define a running coupling with periodic boundary conditions [4]. Unfortunately, this leads to a definition of the coupling that is non-analytic in g_0^2 and thus has a non-universal 2-loop coefficient in the QCD β -function. It considerably complicates the perturbative computations beyond tree-level that are needed to safely relate the Λ -parameter of this scheme to $\Lambda_{\overline{\text{MS}}}$.

As it is known for a long time, this behaviour can be avoided from the start by either using twisted boundary conditions or the Schrödinger functional as finite-volume renormalization scheme [5] where Dirichlet boundary conditions are imposed at the time boundaries. One of the authors was also working on a computation of the gradient flow coupling using twisted boundary conditions and presented its results for the full step-scaling function in $SU(2)$ pure gauge theory [6] that shows a promising accuracy towards a new computation of the running coupling and the Lambda parameter in QCD.

3. The gradient flow coupling in the SF

The Schrödinger functional (SF) is the Euclidean propagation kernel of some field configuration at Euclidean time $x_0 = 0$ to $x_0 = T$ where T is the extent of the finite-volume world in time direction. In the spatial direction, gauge fields have periodic boundary conditions with period L while Dirichlet boundary conditions are imposed to the spatial components of the gauge fields at $x_0 = 0, T$. Accordingly time translation invariance is lost and all physical observables explicitly depend on the Euclidean time. In our setup we are only considering vanishing boundary fields. This means that for a spatial Fourier transformed flow field, $\tilde{B}_\mu(\mathbf{p}, x_0, t)$, one would impose

$$\forall \mathbf{p} : \quad \tilde{B}_k(\mathbf{p}, x_0, t) \Big|_{x_0=0, T} = 0, \quad (3.1)$$

while the boundary condition of the time component emerges through the gauge fixing procedure,

$$\mathbf{p} \neq 0 : \quad \partial_0 \tilde{B}_0(\mathbf{p}, x_0, t) \Big|_{x_0=0, T} = 0, \quad (3.2)$$

$$\mathbf{p} = 0 : \quad \tilde{B}_0(\mathbf{0}, x_0, t) \Big|_{x_0=0} = 0, \quad \partial_0 \tilde{B}_0(\mathbf{0}, x_0, t) \Big|_{x_0=T} = 0. \quad (3.3)$$

This is best seen by starting from the lattice formulation and taking the continuum limit. For additional details we have to refer the interested reader to our paper [7] and references therein.

As mentioned earlier the normalization factor \mathcal{N} is obtained by expanding the flow field and thus the energy density in terms of the bare coupling. At $t > 0$ this reads

$$B_\mu = \sum_{n=1}^{\infty} B_{\mu,n} g_0^n, \quad \langle E(t, x_0) \rangle = \sum_{n=0}^{\infty} \mathcal{E}_n(t, x_0), \quad \text{with } \mathcal{E}_n = \mathcal{O}(g_0^{2+n}), \quad (3.4)$$

$$\text{LO: } \mathcal{E}_0(t, x_0) = \frac{g_0^2}{2} \langle \partial_\mu B_{\nu,1}^a \partial_\mu B_{\nu,1}^a - \partial_\mu B_{\nu,1}^a \partial_\nu B_{\mu,1}^a \rangle, \quad (3.5)$$

and only the leading order (LO) will contribute to \mathcal{N} . Inserting the expansion of B_μ into the flow equation reads to leading order

$$\frac{d}{dt} \tilde{B}_{\mu,1}(\mathbf{p}, x_0, t) = (-\mathbf{p}^2 + \partial_0^2) \tilde{B}_{\mu,1}(\mathbf{p}, x_0, t), \quad \tilde{B}_{\mu,1}(\mathbf{p}, x_0, t) \Big|_{t=0} = \tilde{A}_\mu(\mathbf{p}, x_0), \quad (3.6)$$

which evidently is a heat equation. Solutions to these kind of equations have been known for a long time and can be written in terms of heat kernels. Those that enter our observable can be written as

$$\tilde{B}_{\mu,1}(\mathbf{p}, x_0, t) = e^{-\mathbf{p}^2 t} \int_0^T dx'_0 K^{D,N}(x_0, x'_0, t) \tilde{A}_\mu(\mathbf{p}, x'_0, t), \quad (\mathbf{p} \neq 0) \quad (3.7)$$

where K^D, K^N are heat kernels consistent with *Dirichlet* ($\mu = 1, 2, 3$) and *Neumann* ($\mu = 0$) boundary conditions, respectively, at $x_0 = 0, T$. Inserting these into eq. (3.5) leads to partial derivatives of the heat kernels convoluted with the standard gluon propagator w.r.t. the fundamental gauge fields A_μ . Since the latter is known analytically everything can be written down in closed form and the normalization factor be read-off. In general the continuum normalization factor \mathcal{N} depends on the parameter c , the time-slice used in the evaluation of $E(x_0, t)$ and the geometry that is applied, i.e., the ratio T/L . It is most advantageous to work at $x_0 = T/2$ with $T = L$. Useful choices for c will be discussed below. To ease notation and the discussion of the overall computation we worked in the continuum but the same procedure is carried over to the lattice formulation. There the corresponding norm $\hat{\mathcal{N}}$ will explicitly depend on the lattice size L/a and implicitly on further details as the lattice action and the actual discretisation of the energy density that has been used. In [7] we have done this computation for the Wilson plaquette gauge action and the clover definition of the energy density. Our results have also been checked by using some dedicated small coupling simulations that show the correct asymptotic behaviour.

4. Non-perturbative results

To immediately learn more about the general non-perturbative behaviour of the gradient flow coupling in the SF as defined earlier we decided to compute the corresponding observable $E(x_0, t)$ for different values of the smearing ratio c on existing $N_f = 2$ gauge field configurations for lattice sizes $L/a = 6, 8, 10, 12, 16$ with $T = L$. These have been set up along a trajectory in the space of bare couplings at which the traditional SF coupling and PCAC quark mass are fixed to

$$\text{LCP:} \quad \bar{g}_{\text{SF}}^2(L_1) \equiv u = 4.484 \quad \text{and} \quad m(L_1) = 0, \quad (4.1)$$

corresponding to a physical box size of $L_1 \sim 0.4 \text{ fm}$. Our observable of interest thus reads

$$\Omega(u; c, a/L) = \left[\hat{\mathcal{N}}^{-1}(c, T/L, x_0/T, a/L) \cdot t^2 \langle E(T/2, t) \rangle \right]_{t=c^2 L^2/8}^{\text{LCP}} \quad (4.2)$$

and we show some selected data in figure 1. There the by far dominating part of the overall error budget ($\gtrsim 85\%$) comes from propagating the uncertainty of setting up a line of constant physics (LCP) according to (4.1). The continuum limit is taken without the coarsest lattice $L/a = 6$. We observe the following: (a) below $c = 0.3$ we see deviations from the naive leading scaling expectation (a^{-2}) that gets stronger and stronger with decreasing smearing range, (b) in the range $0.3 \leq c \leq 0.5$ relative cutoff effects stay below 10% and decrease with increasing c , (c) the uncertainty increases with increasing smoothing range.

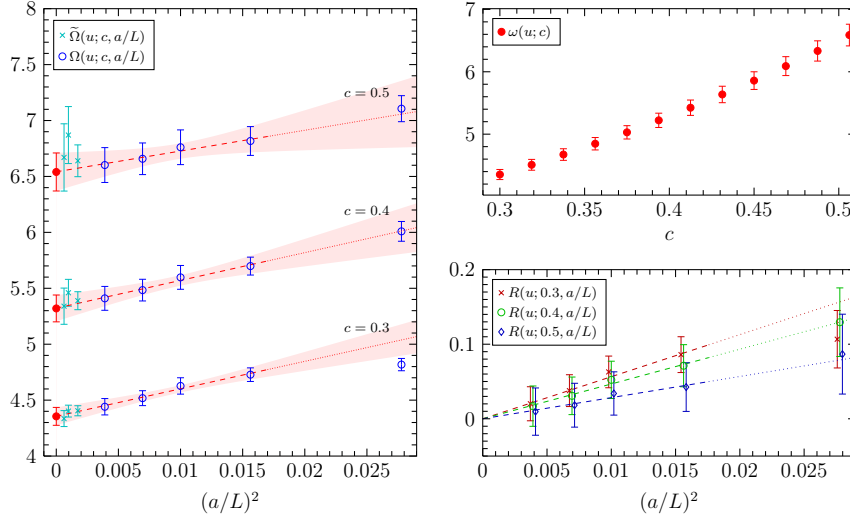


Figure 1: Exemplary results of $\Omega(u; c, a/L)$ with continuum limits $\omega(u; c)$ and its dependence on c .

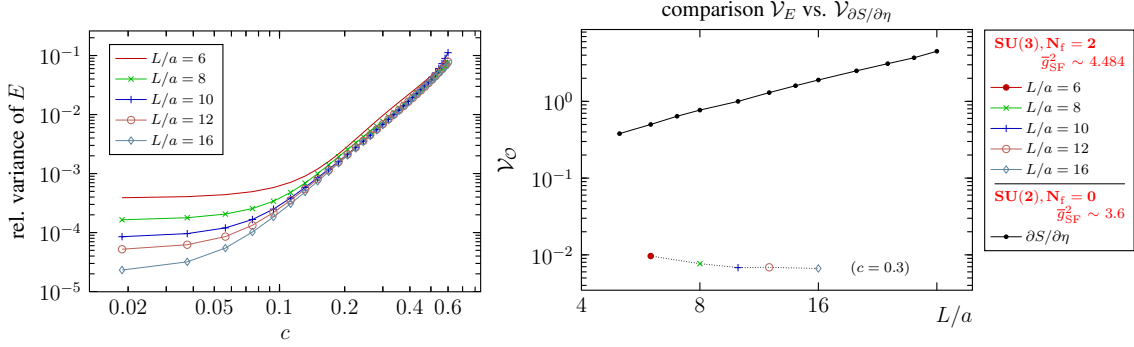


Figure 2: Relative variance of the SF gradient flow coupling compared to that of the traditional SF coupling.

The relative variance

In order to judge how accurately the continuum limit can be reached with the SF gradient flow coupling compared to the traditional SF coupling, we also computed the relative variance that for any observable \mathcal{O} is given by

$$\mathcal{V}_{\mathcal{O}} = \frac{\langle \mathcal{O}^2 \rangle - \langle \mathcal{O} \rangle^2}{\langle \mathcal{O} \rangle^2}. \quad (4.3)$$

Since numerical prefactors cancel one has $\mathcal{V}_{\bar{g}_{\text{GF}}^2} = \mathcal{V}_E$. Note that $\mathcal{V}_{\mathcal{O}}$ is a genuine observable that tells us about the statistical accuracy that can be achieved for an observables \mathcal{O} when the continuum limit is approached in contrast to the integrated autocorrelation time $\tau_{\text{int}, \mathcal{O}}$ that tells us how the underlying algorithm performs for this observable.

The results for our five lattices are shown in the left panel of figure 2. As we have noted earlier one wants to avoid—or is unable—to take the continuum limit for $c \ll 0.3$ due to large cutoff effects and it seems that for say $c > 0.2$ the variances $\mathcal{V}_E(a/L)$ fall onto a universal curve. A similar study has been done for the SF coupling in the case of pure $SU(2)$ gauge theory [8], showing that the variance of the SF coupling diverges towards the continuum limit. In the right

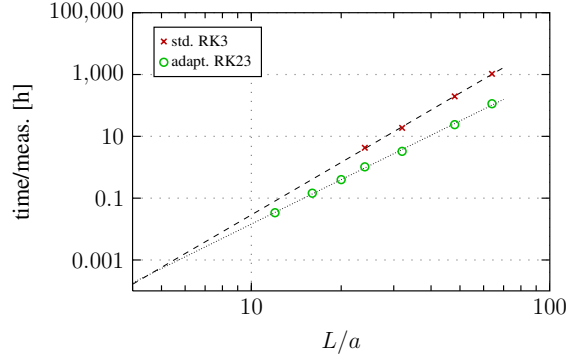


Figure 3: Scaling behaviour of standard Runge-Kutta integrator (RK3) [1] versus adaptive step-size integrator (RK23) [7] for an equivalent setup integrated up to $c_{\max} = 0.5$

panel of figure 2 we plot their results from table 1 together with our result for the SF gradient flow coupling at $c = 0.3$. Note that both are obtained along a line of constant physics defined through a large but slightly different SF coupling and that the overall behaviour of the SF coupling is the same in QCD with dynamical flavours as studied in the case of the gradient flow coupling.

The integrated autocorrelation time of \bar{g}_{GF}^2

Our statistical errors always include an estimate of the integrated autocorrelation time using the Γ -method [9] and we observe a scaling of

$$\tau_{\text{int}, \bar{g}_{\text{GF}}^2} \Big|_{c=0.3} \approx (L/a)^2 \times 0.05 \text{ MDU} \quad (4.4)$$

that agrees with the scaling behaviour that is naively expected for a Hybrid Monte Carlo simulation ($\propto a^{-2}$). At finite flow time also the topological charge can be measured much more accurately and one could ask how the different topological sectors couple to \bar{g}_{GF}^2 , especially in physically larger lattices, i.e., in the low energy regime of QCD. This question is directly related to critical slowing down and was studied in more detail in [10].

Scaling of the numerical Wilson flow integrator scheme

In order to integrate the associated flow equations, a first-order differential equation in the gauge group, the Euler or any Runge-Kutta scheme can be used. In [7] we extend the originally proposed Runge-Kutta scheme (RK3) with fixed step-size [1] by nesting a 2nd order scheme to define an adaptive step size scheme (RK23). Due to the smoothing property of the flow the step size is safely increased with flow time. For simulations that we are currently performing with lattices up to $L/a = 64$ we have collected the run time for measurements of Wilson flow observables up to a fixed flow time and identical setup. The results are plotted in figure 3 and it can be easily inferred that for the largest lattice a speed-up factor of ~ 10 is seen. Already on a $L/a = 32$ lattice, which may typically be used for the finest resolution in a step-scaling procedure, a significant speed-up is achieved.

5. Conclusions & Outlook

We have perturbatively computed the continuum and lattice behaviour of the energy density at positive gradient flow time in the Schrödinger functional with vanishing boundary fields [7]. This allows us to define a new finite-volume renormalization scheme. From our studies we see that for wisely chosen flow parameter ($0.25 \lesssim c \lesssim 0.5$) a controlled continuum limit can be taken. Furthermore, we find strong numerical evidence that the new coupling can be computed with high accuracy. We also observe that the variance of the coupling is independent of L/a which will improve continuum determinations of observables such as the Λ -parameter. This new non-perturbative coupling may also be very useful in the search for a conformal window in beyond the standard model theories.

However, due to the highly improved statistical accuracy there are still many corners to explore. For instance, in the past perturbatively computed boundary improvement terms like c_t and \tilde{c}_t were not affecting the results or error budget. We are currently investigating such issues with the tree-level improved Lüscher-Weisz gauge action.

Acknowledgments

This work is supported in part by the Deutsche Forschungsgemeinschaft under SFB/TR 9. We gratefully acknowledge the computer resources provided by the John von Neumann Institute for Computing as well as at HLRN and at DESY, Zeuthen.

References

- [1] M. Lüscher, *Properties and uses of the Wilson flow in lattice QCD*, *JHEP* **1008** (2010) 071, [[1006.4518](#)].
- [2] M. Lüscher and P. Weisz, *Perturbative analysis of the gradient flow in non-abelian gauge theories*, *JHEP* **1102** (2011) 051, [[1101.0963](#)].
- [3] M. Lüscher, *Trivializing maps, the Wilson flow and the HMC algorithm*, *Commun.Math.Phys.* **293** (2010) 899–919, [[0907.5491](#)].
- [4] Z. Fodor, K. Holland, J. Kuti, D. Nogradi, and C. H. Wong, *The Yang-Mills gradient flow in finite volume*, *JHEP* **1211** (2012) 007, [[1208.1051](#)].
- [5] M. Lüscher, R. Narayanan, P. Weisz, and U. Wolff, *The Schrödinger functional: A Renormalizable probe for non-Abelian gauge theories*, *Nucl.Phys.* **B384** (1992) 168–228, [[hep-lat/9207009](#)].
- [6] A. Ramos, *The gradient flow in a twisted box, these proceedings* (2013).
- [7] P. Fritzscher and A. Ramos, *The gradient flow coupling in the Schrödinger Functional*, [1301.4388](#).
- [8] ALPHA Collaboration, G. de Divitiis *et. al.*, *Universality and the approach to the continuum limit in lattice gauge theory*, *Nucl.Phys.* **B437** (1995) 447–470, [[hep-lat/9411017](#)].
- [9] N. Madras and A. D. Sokal, *The Pivot algorithm: a highly efficient Monte Carlo method for selfavoiding walk*, *J.Statist.Phys.* **50** (1988) 109–186.
- [10] P. Fritzscher, A. Ramos, and F. Stollenwerk, *Critical slowing down and the gradient flow coupling in the Schrödinger functional, these proceedings* (2013).